Water Research 214 (2022) 118197

Contents lists available at ScienceDirect

Water Research

journal homepage: www.elsevier.com/locate/watres

Novel insights into molecular composition of organic phosphorus in lake sediments

Zhaokui Ni [a,b,c], Dongling Huang [d], Yu Li [a,b,c], Xiaofei Liu [a,b,c], Shengrui Wang [a,b,c,e,*]

[a] Guangdong-Hong Kong Joint Laboratory for Water Security, Center for Water Research, Advanced Institute of Natural Sciences, Beijing Normal University at Zhuha, Beijingi, 519087, China
[b] College of Water Sciences, Beijing Normal University, Beijing 100875, China
[c] Engineering Research Center of Ministry of Education on Groundwater Pollution Control and Remediation, College of Water Sciences, Beijing Normal University, Beijing 100875, China
[d] College of Resource Environment and Tousism, Capital Normal University, Beijing 100048, China
[e] Yunnan Key Laboratory of Pollution Process and Management of Plateau Lake Watershed, Kunming 650034, China

ARTICLE INFO

Keywords:
^{31}P NMR
Molecular weight
Composition
Organic phosphorus
Lake sediment

ABSTRACT

Organic phosphorus (P_o) plays a key role in eutrophication and ecological equilibrium in lake systems. However, characterizing the composition of P_o in lake sediments has been a bottleneck hindering further understanding of the biogeochemical cycle of P_o. Here, multiple methods of ^{31}P NMR spectroscopy and molecular weight (MW) ultrafiltration were combined to detect P_o composition characteristics from a novel angle in ten lake sediments of China. The results showed that sediment P_o mainly consisted of monoester (mono-P, 14±8.8% of the NaOH-EDTA total P on average), diester (di-P, 1.4±1.4%) and phosphonate (phos-P, 0.1±0.1%), while the abundance of P_o was largely underestimated by ^{31}P NMR methods. Some specific species of mono-P were successfully determined, and the contents of these species followed a decreasing order: inositol hexakisphosphate (IHP6) > RNA mononucleotides (RNA-mnP) > β-glycerophosphate (β-gly) > D-glucose 6-phosphate (Glu-6) > α-glycerophosphate (α-gly), which was largely dependent upon their bioreactivity. A significant relationship between MW and P_o components was observed despite the great differences among sediment samples. For refractory P_o components, IHP6 was mainly rich in the MW < 3 kDa while phos-P was almost only detected in the MW > 3 kDa, which largely attributed to their metal binding affinities and characteristics. The abundance of bioreactive P_o species (α-gly, β-gly, Glu-6, di-P) in high MW (HMW, > 3 kDa) were all higher than that of low MW (LMW, < 3 kDa) due to microbial degradation and self-assembly. If the HMW organic molecules were biologically and chemically more reactive than its LMW counterparts, the high percentage of α-gly, β-gly, glu-6 and di-P in the HMW portion would highlights their high reactivity from the perspective of MW. These insights revealed the dynamics of the MW distribution of P_o components and provide valuable information to better understand the P_o composition and bioreactivity in sediments.

1. Introduction

The release of phosphorus (P) loading from sediment is a worldwide concern as it causes the instability of aquatic ecosystem and accelerate lake eutrophication (Wu and Wang, 2017 Horppila; et al., 2019). Accurate estimation of internal P loading from sediments is important for water quality risk assessment and lake management (Rippey et al., 2021). It has been widely recognized that internal P loading can trigger a positive feedback of lake eutrophication (Orihel et al., 2017; Tu et al., 2021), in which the release of inorganic (P_i) and the degradation of organic P (P_o) produce orthophosphate through chemical decomposition, photodegradation and biomineralization processes (Søndergaard et al., 2003; Ahlgren et al., 2011; Li et al., 2019; Li et al., 2021). However, due to the complex composition of P_o and to the limitation of analytical technologies (Venkatesan et al., 2018), the contribution of P_o to internal P loading has not been well understood. As one of the major parts of P in the environment, P_o is a complex mixture where P is integrated into organic matter and forms different fractions (Bedrock et al., 1995 Worsfold et al., 2008; Cade-Menun, 2005; Ding et al., 2010). With an increasing attention on P_o and advanced analytical techniques, a few studies have demonstrated that P_o are highly bioavailable (Zhu et al.,

* Corresponding author at: Beijing Normal University - Zhuhai Campus, China.
E-mail address: wangsr@bnu.edu.cn (S. Wang).

https://doi.org/10.1016/j.watres.2022.118197
Received 24 November 2021; Received in revised form 8 February 2022; Accepted 13 February 2022
Available online 14 February 2022

Nomenclature

MW	Molecular weight
HMW	High molecular weight
LMW	Low molecular weight
kDa	Kilo Dalton
P_o	Organic phosphorus
P_i	Inorganic phosphorus
EDTA	Ethylenediamine tetraacetic acid
Mono-P	Monoester P
Di-P	Diester P
Phos-P	Phosphonate
α-gly	α-glycerophosphate
β-gly	β-glycerophosphate
Glu-6	D-glucose 6-phosphate
IHP6	Inositol hexakisphosphate
RNA-mnP	RNA mononucleotides

2013; Ni et al., 2016; Zhang et al., 2017; Feng et al., 2018). Studies have reported that P_o could be utilized concurrently with inorganic P as a P source to aquatic ecosystems, and its nutrient value is greater when total P supplies are limited (Björkman and Karl, 2003; Ruttenberg and Dyhrman, 2005). Although studies on the abundance, composition, circulation and characteristics of P_o have been widely investigated, the structural and compositional characterization of P_o at molecular level remains missing, thus restricting the estimation of P_o species that contribute to internal P loadings.

The complexity and lack of compositional information on P_o in sediments, hampers our understanding of its bioreactivity, fates and environmental implications. Among numerous analytical techniques for identifying the species of P_o compounds in sediments and soil (Ivanoff, et al., 1998; Liu et al., 2013; Venkatesan et al., 2018; Hurtarte et al., 2020; Ni et al., 2021), ^{31}P NMR spectroscopy is most frequently used due to its comprehensive and non-destructive performance (Cade-Menun, 2005; Worsfold et al., 2008). The ^{31}P NMR spectroscopy method can identify specific P_o species, including inositol phosphates, sugar phosphates, DNA and RNA fragments, phospholipids, phosphate esters, etc. (Wu and Xing, 2009; McLaren et al., 2015a; Giles et al., 2015).

As a basic feature of dissolved organic molecules, MW is usually closely related with their chemical compositions. McLaren et al (2015b) demonstrated that the speciation of P_o in soil have a great variation in MWs. HMW dissolved organic molecules usually have stronger bindings to metal ions than that of LMW ones (Lakshman et al., 1993; Christl and Kretzschmar, 2001; Chen et al., 2013; Xu et al., 2019), and hence influence the bioreactivity of specific P_o components, such as phosphonate and inositol hexaphosphate metal compounds. MW is also an important factor influencing the bioreactivity of dissolved P_o in the environment. Studies have shown that the bulks of high MW (HMW) dissolved organic molecules are more bio-reactive, therefore can be more rapidly utilized by microbes than those with low MW (LMW) (Amon and Benner, 1994; Arnosti et al., 1994; Amon and Benner, 1996; Benner and Amon, 2015). Hence, studying the MW distribution of P_o composition might shed light on the internal mechanism about the bioreactivity of P_o in sediments.

Sediment systems are of high heterogeneity in terms of the composition of P_o compounds. Specifically, the compounds with different MWs exhibit distinctive characteristics in content and abundance (Ged and Boyer 2013; McLaren et al., 2015b), which in turn influence their reactivities and fates. However, current knowledge on the MW distribution for different components of P_o in sediments remains unclear. Thus, there is an urgent need to explore the response of MW fraction to the composition of P_o in sediments.

In this study, the NaOH-ethylenediaminetetraacetic acid (EDTA) method was used to efficiently extract P_o (Cade-Menun and Preston, 1996; Turner et al., 2003a), while ^{31}P NMR and MW ultrafiltration were combined to explore the MW distribution characteristics of each identified P_o components using samples of ten lakes from the Eastern Plain and Yunnan-Guizhou Plateau of China. Additionally, the plausible explanations for the MW distribution of P_o components and environmental implications were discussed. This study is expected to provide further insights about the compositional characteristics of P_o at molecular level.

2. Material and methods

2.1. Study sites and sample collection

The Eastern Plain and Yunnan-Guizhou Plateau in China possess a vast number of lakes, most of which face eutrophication risks. Ten lakes from those regions were selected as the study sites (see Fig. 1). Among the selected lakes from the Eastern Plain, some are located at middle and lower reaches of Yangtze River and Huai River, others at lower reaches of Yellow River and Hai River, or along the Beijing-Hangzhou Grand Canal. Most of the lakes are shallow with the eutrophication being a major concern (Le et al., 2010). Lake Baiyang (ID: BY, sampling site at 38°56′3.84"N, 116°0′23.04"E), Lake Hengshui (HS, 37°37′28.9''N, 115°36′57''E), Lake Dianshan (DS, 31°7′14.16"N, 120°57′25E), Lake Poyang (PY, 28°59′5″N, 116°19′23″E), Lake Taihu (TH, 31°6′39"N, 120°2′31"E), and Lake Wuhan-Dong (WD, 30°34′38″N, 114°23′59″E) were selected in this area, with trophic level index being 58, 51, 59, 51, 58, and 65, respectively (Chinese Ecological Environment Bullet, 2018). Lakes in Yunnan-Guizhou Plateau mainly located in the middle of the area, where the Lake Dianchi (DC, 24°52′14"N, 102°43′29"E), Lake Yilonghu (YLH, 23°39′26″N, 102°36′32″E), Lake Erhai (EH, 25°40′5.88"N, 100°13′58.8"E) and Lake Lugu (LG, 27°42′44"N, 100°46′50"E) were selected, whose trophic level index is 58, 61, 42 and 14, respectively.

Overall, these sampling sites are in remote areas with little influence from anthropogenic activities, therefore they can represent the natural states of the lake environment. In addition, the selected lakes are characterized by distinctive climatic regimes, as well as by the spatial heterogeneity in water depths and trophic levels. Analysis based on the samples of those lakes can better capture the general patterns in P_o's composition as well as MW distribution, therefore enabling more general conclusions.

In total, ten surface sediment samples from ten lakes were collected in August and September 2018 (Fig. 1). At each sampling site, the sediments were first obtained by a columnar sampler. Then the sediments from the bottom of the lakes down to a depth of 5 cm were collected into sealed dark plastic bags and kept at 4 °C. In laboratory, the sediments were freeze-dried and grounded through a 100-mesh (0.149 mm) sieve after removing gravels and plant fragments.

2.2. NaOH−EDTA extraction

NaOH−EDTA extraction can provide a close estimate to the total extractable P, facilitating the subsequent P_o characterization with ^{31}P NMR spectroscopy (Cade-Menun and Preston, 1996). 2 g dried sediments were extracted with 50 mL of sodium hydroxide−ethylenediaminetetraacetic acid mixture (0.25 M NaOH + 25 mM EDTA) at 25 °C. After 16 h of oscillation, extracts were centrifuged at 5, 000 r/min for 15 min and then the supernatants were passed through a 0.45 μm glass filter (Keyilong Experimental Equipment Co., Ltd, Tianjin, China) preheated for 3 h at 450 °C.

A portion of the extract was used for MW ultrafiltration. The rest were used to measure the content of the NaOH-EDTA extractable total P and the NaOH-EDTA extractable P_i. The NaOH-EDTA extractable total P was measured by the molybdenum blue/ascorbic acid method after digestion, while the NaOH-EDTA extractable P_i was direct measured by molybdenum blue/ascorbic acid method without digestion. The NaOH-EDTA extractable P_o was calculated as the difference between the

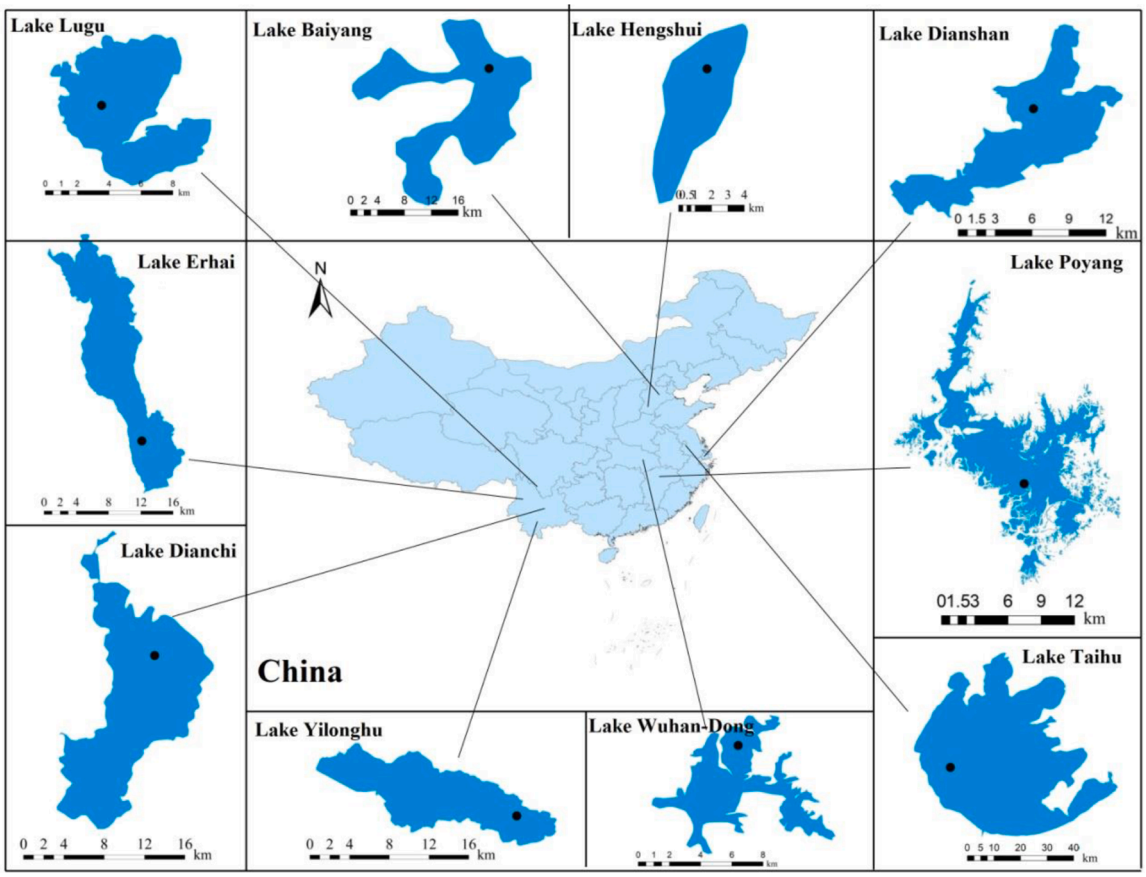

Fig. 1. The location of sampling sites in the Yun-Gui Plateau and Eastern Plain lakes of China.

NaOH-EDTA extractable total P and the NaOH-EDTA extractable P_i.

The analysis of the total P content in sediment was performed following the European testing standards (Ruban et al., 1999). The extraction rate with NaOH-EDTA was calculated as the NaOH-EDTA extractable total P divided by the total P in sediments.

2.3. MW ultrafiltration

The NaOH-EDTA extract was transferred to an ultrafiltration device (model 8400 , Millipore Corporation, Massachusetts, USA) containing 10 kDa, 3 kDa and 1 kDa filtration membranes made of regenerated cellulose (model YM, Millipore Corporation). The extract was successively passed through 10 kDa, 3 kDa and 1 kDa filter membranes to reduce concentration difference which could affect the subsequent filtering processes. The NaOH-EDTA extractable total P was divided into four MW groups after ultrafiltration (Zhang et al., 2016), namely > 10 kDa, 3-10 kDa, 1-3 kDa and <1 kDa, respectively. Each MW group was defined as follows:

$$\omega(>10\text{kDa}) = \omega(\text{raw}) - \omega(<10\text{kDa}) \quad (1)$$

$$\omega(3-10\text{kDa}) = \omega(<10\text{kDa}) - \omega(<3\text{kDa}) \quad (2)$$

$$\omega(1-3\text{kDa}) = \omega(<3\text{kDa}) - \omega(<1\text{kDa}) \quad (3)$$

where ω (< 10 kDa), ω (< 3 kDa) and ω (< 1 kDa) represents the concentration of the NaOH-EDTA extractable total P in the components of < 10 kDa, < 3 kDa, and < 1 kDa, respectively.

2.4. Solution ^{31}P NMR spectroscopy

The filtrate of each MW fraction was freeze-dried to powder. The solid samples were dissolved in a solvent prepared with 1 mL of 1M NaOH, 0.1 mL of deuterium oxide (D_2O) and 0.1 mL of 1 M Na_2S, and then treated by ultrasonification for 30 min. Next, the mixture was kept for 24 hours at 4 °C. Then it was filtered and placed in a 5 mm NMR tube. Solution ^{31}P NMR spectra were analyzed at 161.98 MHz on a BRUKERAV-600 MHz NMR spectrometer equpiped with a 5 mm broad band probe. The spectrometer was configured with 12 microsecond acquisition time, 5 Hz spinning speed, 5 second relaxation delay, and 6,400 accumulated scans.

The peak areas were calculated by integrating over predetermined spectral regions using MestReNova 9.0 software (Mestrelab Res Co, Spain). P species with different MWs were identified by comparing their chemical shifts with those of standardized ones. 85% H_3PO_4 was used as an external standard. Each NaOH-EDTA extractable P components showed a distinct chemical shift: orthophosphate (orth-P, 5 to 7 ppm), pyrophosphate (pyro-P, −4 to −5 ppm), orthophosphate monoesters (mono-P, 3 to 6 ppm), orthophosphate diester (di-P, −1 to 2.5 ppm), and phosphonate (phos-P, 19 to 24 ppm) (Cade-Menun et al., 2005; Wu and Xing, 2009). Mono-P can be further divided into α-glycerophosphate (α-gly, 4.9 ppm), β-glycerophosphate (β-gly, 4.6 ppm), D-glucose 6-phosphate (Glu-6, 5.14 to 5.34 ppm), RNA mononucleotides (RNA-mnP, 4.0, 4.1, 4.5, 5.4, ppm), inositol hexakisphosphate (IHP6, 4.7, 4.4, 4.2, 3.9 ppm) and other mono-P components (McLaren et al., 2015b). Di-P includes lipid P (0 to 2 ppm), RNA (1.9 to -0.2 ppm), DNA (-0.36 ppm) and other di-P (Feng et al., 2018). The relative abundance of each P species was calculated as its individual peak area divided by the total detected peak area.

3. Results and discussions

3.1. Identification of sediment P_o composition

As shown in Fig. 2a, the NaOH-EDTA extraction rate of the total P ranged between 23% and 63% (45±12.7% on average), which is similar to the results reported for sediments and soil samples (Shinohara et al., 2012; Zhang et al., 2013). The non-extractable P such as refractory P_o (e.g., phytate P) and immobile P_i (e.g., Ca-bound P) might not be bioavailable (Bowman and Cole, 1978; Shinohara et al., 2012). The NaOH-EDTA extractable P species, including orth-P, mono-P, di-P, pyro-P and phos-P, were determined in the raw sediments by ^{31}P NMR peaks (Fig. S1). Di-P was not detected at BY, PY, TH, DC sampling sites,

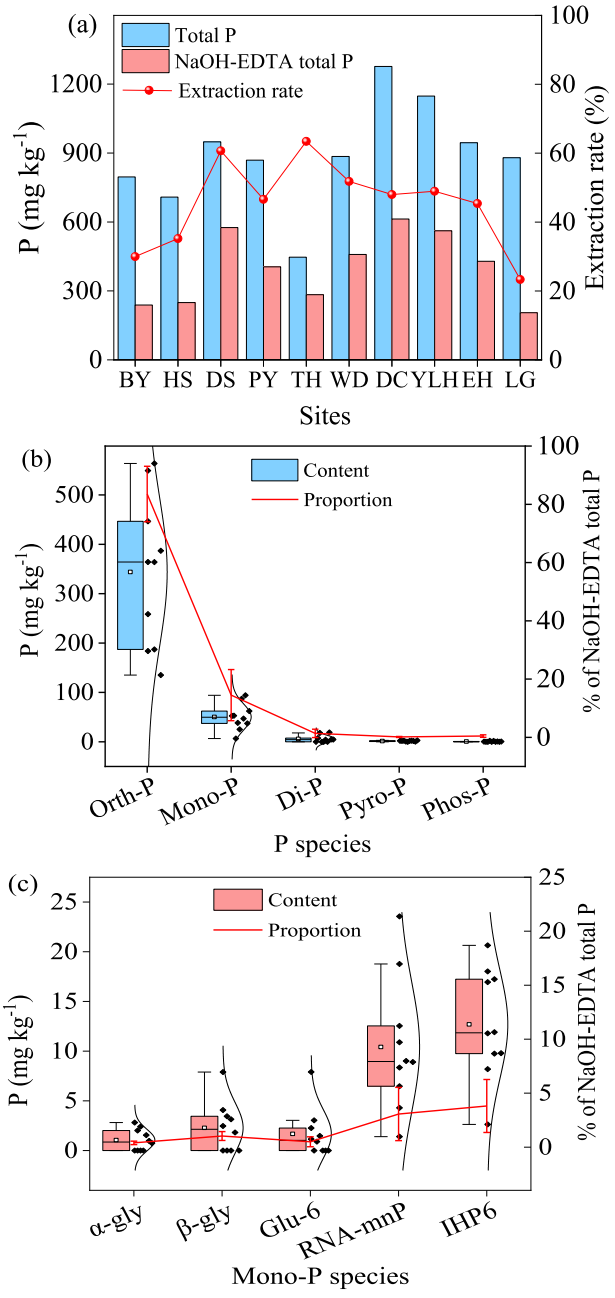

Fig. 2. Extraction rate of total P (a), and the content and percentage of each species P (b) and Mono-P (c) compounds in NaOH-EDTA extracts from the lake sediments. The box and whisker plots show the mean (square), median (horizontal line), 25th and 75th percentile (lower and upper edge of box), and the 5th and 95th percentile (lower and upper whisker).

which could be attributed to its high bioreactivity. Di-P can be easily transformed into orth-P and mono-P as a result of the degradation of enzyme and microorganisms, as well as the chemical hydrolysis during the alkaline extraction pretreatment of ^{31}P NMR (Makarov et al., 2002; Ahlgren et al., 2006a; Shinohara et al., 2012).

The content of the NaOH-EDTA extractable P components in raw sediments, as derived from NMR peak areas (Fig. 2b), showed a decreasing order: orth-P (66–95% of NaOH-EDTA total P) > mono-P (1–30%), di-P (0–3%) > pyro-P (0–1%) > phos-P (0–0.5%), with an average portion of 84±9.5%, 14±8.8%, 1.4±1.4%, 0.5±0.4% and 0.1 ±0.1%, respectively. Compared with the NaOH-EDTA P_i content, the content of orth-P (^{31}P NMR) all had higher values except for the sample at LG, with a ratio of orth-P (^{31}P NMR) over the NaOH-EDTA extractable P_i ranging between 0.89 and 1.58 (1.21±0.23 on average) (Fig. S2). In contrast, the content of P_o (i.e., sum of mono-P, di-P and phos-P by ^{31}P NMR) all had lower values than that of the NaOH-EDTA extractable P_o except for the samples at LG, with the ratio of orth-P over the NaOH-EDTA extractable P_o ranging between 0.20 and 1.23 (0.59±0.35 on average). These results indicate that the alkaline condition and the enrichment process of NaOH-EDTA extraction in the ^{31}P NMR pretreatment would cause chemical degradation of P_o compounds. Since the chemical shift of ^{31}P NMR spectra is sensitive to pH and salt, lyophilization in NaOH-EDTA can hydrolyze P_o, leadingg to the increase of orth-P release from P compounds (Turner et al., 2003a; Barbara et al., 2006; Zhang et al., 2014). As a consequence, characterizing P_o using ^{31}P NMR method would underestimate the content of P_o in lake sediments.

Several compounds, namely α-gly, β-gly, RNA-mnP, Glu-6 and IHP6 were detected in the mono-P range by ^{31}P NMR (Fig. 2c & Fig. S3). α-gly and β-gly are usually recognized as the products from phospholipids degradation (Turner et al., 2003a; Doolette et al., 2009; He et al., 2011; Feng et al., 2016), representing the labile mono-P. Results showed that α-gly only accounts for 0–0.7% (0.4±0.1% on average) of the NaOH-EDTA extractable total P, and β-gly accounts for 0–1.5% (1.0 ±0.4% on average). Glu-6 is involved in biochemical reactions of pentose phosphate and glycolysis (Feng et al., 2016), which can easily be utilized by microorganisms, and accounts for 0–1.4 % (0.5±0.5% on average) of the NaOH-EDTA total P. RNA-mnP is generally considered as the products from RNA degradation (Turner et al., 2003a; Bünemann et al., 2008), which occurs in sediments and water (Ahlgren et al., 2006b; Reitzel et al., 2007). Results showed that RNA-mnP is the second dominating mono-P form, accounting for 0.3–9.1% (3.1±2.5% on average) of the NaOH-EDTA extractable total P in sediments, consistent with the results reported in the study in Lake Kasumigaura, where the mnP accounted for the largest portion of P_o in suspended particles (Shinohara et al., 2016). IHP6 in sediments has been shown to be recalcitrant (Turner et al., 2003b; Turner and Weckström, 2009; Jørgensen et al., 2011), and it is the dominant form of mono-P, accounting for 0.5–8.4% (3.8±2.4% on average) of the NaOH-EDTA extractable total P. The content of mono-P components followed an increasing order: labile part (α-gly, Glu-6, β-gly, RNA-mnP) < non-labile part (IHP6) parts, suggesting that the content of mono-P components in sediments largely depends upon their bioreactivity.

3.2. MW abundances and distribution of sediment P_o components

MW is a key physicochemical property of organic molecules, but the relationship between P_o compositional characteristics and their MW distribution in sediments is largely unknown. The combination of MW ultrafiltration and ^{31}P NMR method provides a mean to characterize the MW distribution of P_o components. The NaOH-EDTA extractable total P was mainly in < 1 kDa portion, with an average relative abundance of 62% ± 15% (Fig. 3a & Fig. S4a). In comparison, the relative abundance in > 10 kDa, 3-10 kDa and 1-3 kDa fraction was 13%±11%, 11% ± 11% and 14% ± 10% on average, respectively, showing little difference among the MW fractions. These results indicated that the majority of the NaOH-EDTA extractable total P in sediments falls into the LMW fraction

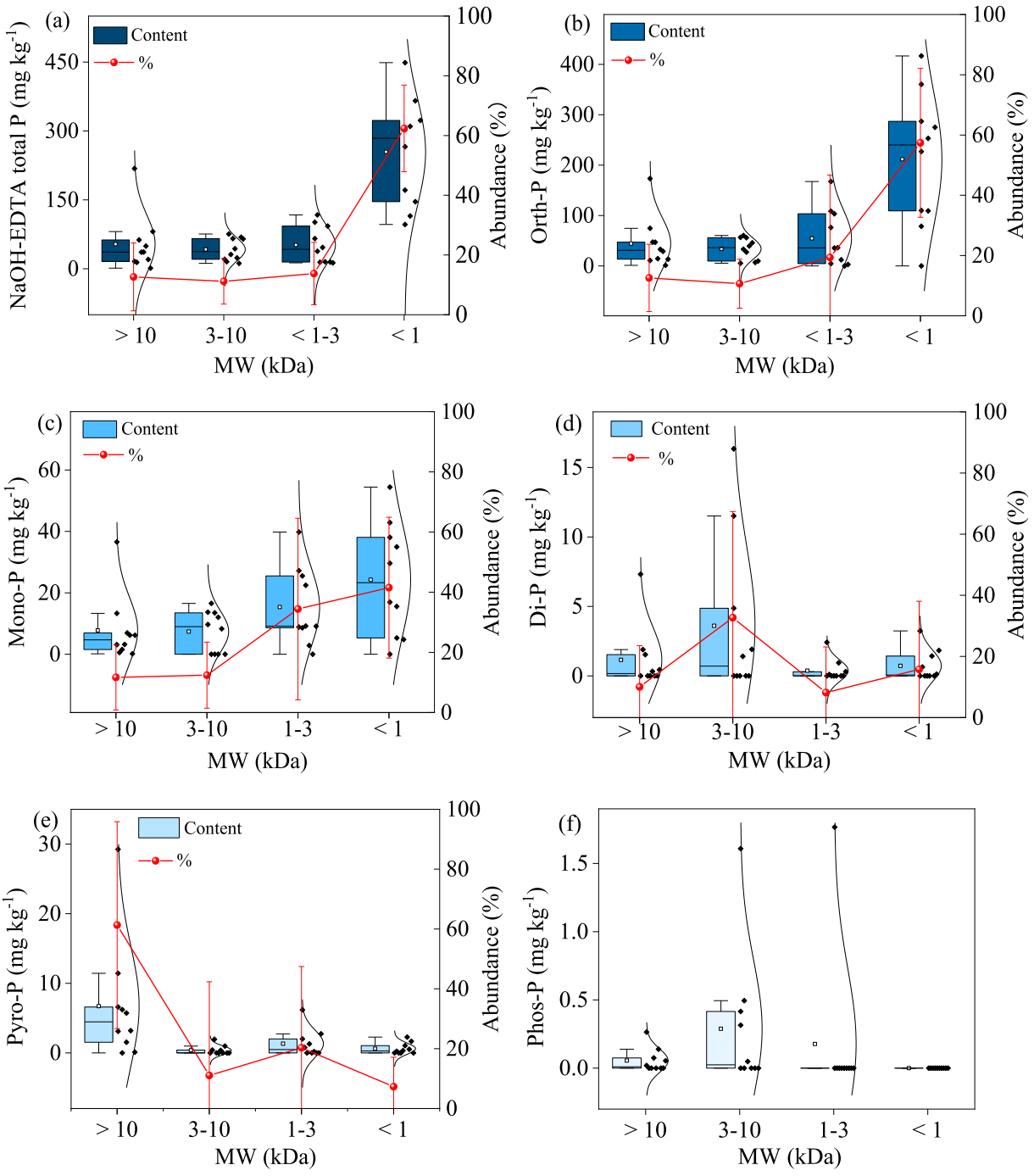

Fig. 3. Content and relative abundance changes with the different MW fractions of the NaOH-EDTA extractable total P (a) and each P species (b: orth-P, c: mono-P, d: di-P, e: pyro-P, f: phos-P).

(< 1 kDa).

Similar to NaOH-EDTA extractable total P, orth-P was mainly contained in the LMW portion, with 57% ± 25% of orth-P on average in < 1 kDa group (Fig. 3b & Fig. S4b). The rest of the fractions accounted for 13% ± 11% in > 10 kDa, 11% ± 8% in 3-10 kDa, and 19% ± 27% in 1-3 kDa, respectively. This is consistent with the results of Venkatesan et al. (2018) and Yang et al. (2021), who found 74–100% of orth-P in LMW (400–600 Da) portion in lake water, and that orth-P was exclusively present in the < 1 kDa part in open bay water. This is largely attributed to inorganic nutrient which can be consumend during bacterial degradation of the HMW fraction and then turn into the LMW fraction (Amon and Benner, 1996). Pyro-P, commonly representing labile P, can be utilized directly by aquatic organisms (Read et al., 2014) or be easily transformed to orth-P in the presence of alkaline phosphatase (Reitzel et al., 2006; Ahlgren et al., 2006a). In this study, pyro-P was concentrated in the HMW portion, with the MW > 10 kDa portion accounting for 61% ± 34% of the total pyro-P (Fig. 3e & Fig. S4e). The proportions of the 3-10 kDa, 1-3 kDa and < 1 kDa fractions were 11% ± 31%, 20% ± 27% and 7% ± 10%, respectively. The causes for the pyro-P distribution with the MW fractions might be two-fold: (1) the HMW ester or poly-P can be easily hydrolyzed into pyro-P, since pyro-P is the hydrolysis product of ester or poly-P during the alkaline extraction procedure (Hupfer et al., 1995); (2) the HMW pyro-P may have strong binding affinity on metal ions (Chen et al., 2013; Xu et al., 2019), thus forming

more stable compounds in sediments.

The largest NaOH-EDTA extractable P_o group in all lakes was mono-P (Fig. 2b), which mainly consists of sugar phophates, mononucleotides, phospholipids, degradation production of ribouncleic acid (RNA), and inositol P (Paytan et al., 2003; Turner et al., 2003a, b). The abundance of mono-P increased steadily with the decrease of MW, i. e., 11%±10%, 12%±11%, 34%±30% and 41%±23% for the > 10 kDa, 3-10 kDa, 1-3 kDa and <1 kDa, respectively. This trend can be attributed to the bacterial degradation of the HMW mono-P, which leads to the breakdown of molecular chain and produces more mono-P with small MW. Di-P represents lipid, DNA and RNA-associated P (Makarov et al., 2002; Paraskova et al., 2013), and is relatively homogeneous in MW distribution. The percentage of di-P in > 10 kDa, 1-3 kDa and < 1 kDa is 10% ± 13%, 8% ± 15%, and 16% ± 22%, respectively, while the 3-10 kDa portion reaches 33% ± 35%) among the sampling sites (Fig. 3d & Fig. S4d). This trend indicates that the content of di-P is independent of the MW. This can be explained by the fact that di-P is highly bioreactive since di-P could be easily transformed to orth-P and mono-P (Ahlgren et al., 2006a; Shinohara et al., 2012). Phos-P is highly stable and resistant to chemical hydrolysis due to the C-P bond (Suzumura et al., 1998; Turner et al., 2002), therefore it was only concentrated in the HMW portion (> 10 kDa, 3-10 kDa), whereas none was detected in the LMW

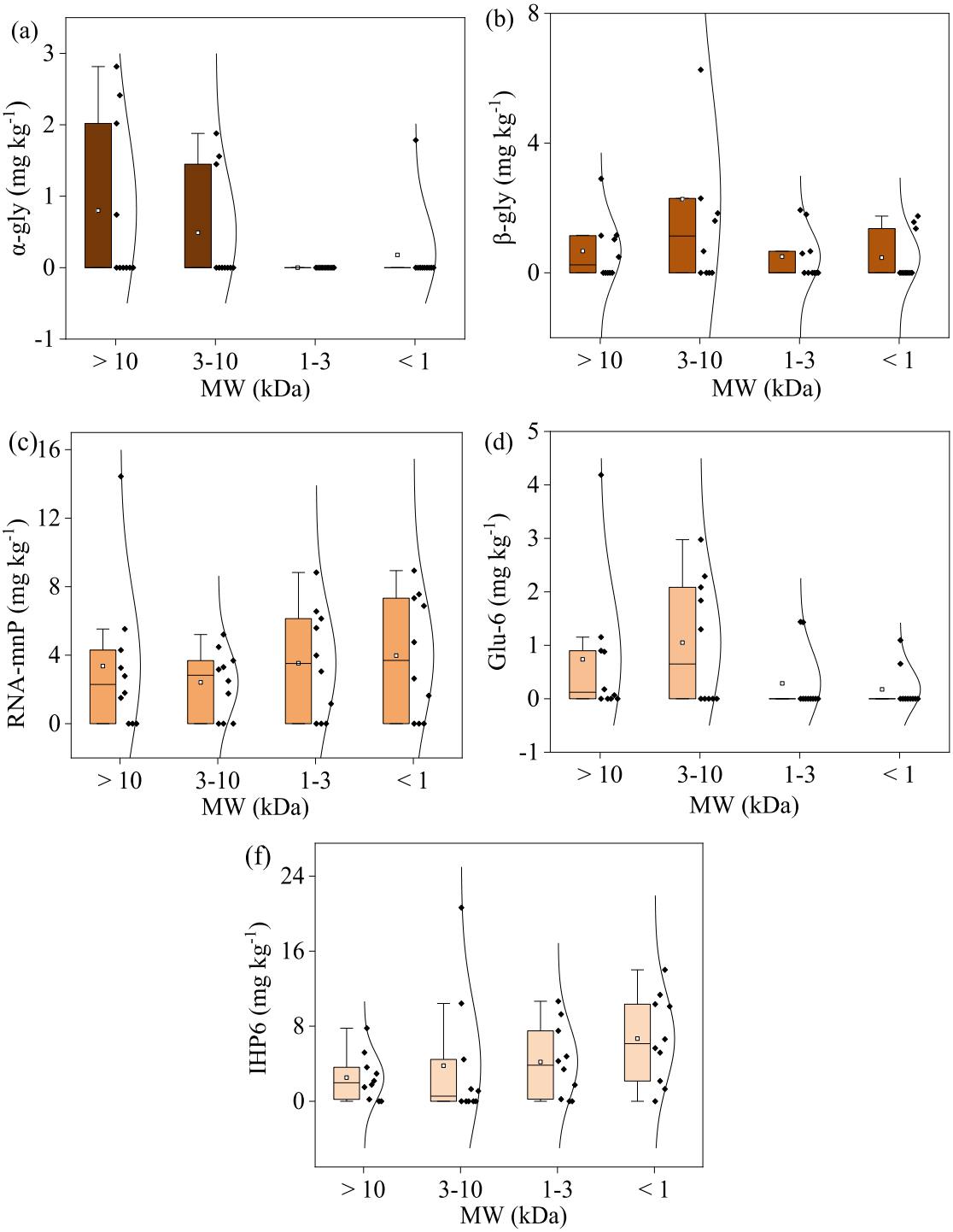

Fig. 4. Content and relative abundance changes with the different MW fractions of each mono-P species (a: α-gly, b: β-gly, c: RNA-mnP, d: glu-6, e: IHP6).

fractions (1-3 kDa, < 1 kDa) (Fig. 3f & Fig. S4f). Phos-P can be effectively integrated with metal ions, showing high structural stability due to metal bond (Silbernagel et al., 2016; Xiong et al., 2019; Weng and Zheng, 2020). The strong binding affinity on metal ions in HMW fractions (Chen et al., 2013; Xu et al., 2019) enhanced the stability of HMW phos-P and hence increased its abundance in sediments.

As shown in Fig. 4 and Fig. S5, the distribution of mono-P species showed great variations with MWs. The NMR peaks, representing α-gly and Glu-6 substances, mainly appeared in the > 10 kDa and 3-10 kDa fractions, while were almost undetectable in the 1-3 kDa and < 1 kDa ones. The RNA-mnP and *β*-gly species showed little dependence on MWs, whereas the amount of IHP6 increased with the increasing MW, namely 2.5±2.4, 3.8±6.8, 4.2±3.9, and 6.7±4.7 mg kg^{-1} for the > 10 kDa, 3-10 kDa, 1-3 kDa, and < 1 kDa fraction, respectively. IHP6 is easily sorbed onto metal ions and forms insoluble metal-phytate (Turner and Weckström, 2009; Jørgensen, et al., 2011). Variations in IHP6 were closely related to simultaneous changes in amorphous metal oxides (Turner et al., 2007; McDowell et al., 2007). Therefore, the strong binding affinity in higher MW (Chen et al., 2013; Xu et al., 2019) would favor insoluble metal-phytate, and thus reduces the accumulation of dissolved IHP6 with higher MW. This explains the increase of IHP6 with decreasing MW.

The linkage between P_o components and MW distribution is important for further understanding the compositional characteristics of P_o in sediments and the subsequent assessment of its bioreactivity. The overall trend of the MW distribution of P_o components showed a general pattern irrespective of the sample difference. A clear dividing point in the MW distribution of P_o components can be seen in the 3 kDa portion (Fig. 5). The high bioreactive P_o species (e.g., *α*-gly, *β*-gly, glu-6, di-P) showed a similar trend with MWs in the sediments, i.e., the relative abundance in the > 3 kDa portion was much higher than that in the < 3 kDa one. Such high percentage of HMW bioreactive P_o species in the sediments may be linked to the source characteristics, microbial degradation and self-assembly of dissolved organic molecules. For example, liberated or freshly photosynthesized dissolved organic molecules usually correspond to HMW materials (Benner and Amon, 2015). Furthermore, Xu and Guo (2018) observed a significant transformation of LMW (< 1 kDa) precursors into colloids (1 kDa - 0.45 μm) and microparticles (> 0.45 μm) during microbial incubation. Kerner et al., (2003) found that diffusion drives aggregation of low- to high-molecular-mass dissolved organic carbon and further to larger micelle-like microparticles. For P_o refractory components, IHP6 mainly existed in the < 3 kDa portion whereas phos-P was rich in the > 3 kDa portion, which could be ascribed to their metal binding characteristics, as discussed in Section 3.2.

3.3. Implications

The characterization of P_o structure and composition is challenging, but is a critical step for understanding the biogeochemical cycles of P. Different approaches were used to analyze size distribution, components, bioreactivity and fates of P_o (Venkatesan et al., 2018; Hurtarte et al., 2020; Kurek et al., 2020; Gao et al., 2021). However, very few studies have examined the molecular size-dependent abundance and composition of P_o in sediments. As a fundamental parameter, MW influences the abundance and composition properties, and thus alters the bioreactivity and fates of P_o.

Here, significant differences in MW distribution of different P_o components were observed. In particular, the abundance of high bioreactive P_o species (e.g., *α*-gly, *β*-gly, glu-6, di-P) in the HMW fraction (> 3 kDa) was much higher than that of LMW (< 3 kDa). If self-assembly made dissolved organic molecules more readily available to phagotrophic organisms (Xu and Guo, 2018), and if the HMW or colloidal ones were biologically and chemically more reactive than its LMW counterparts (Guo et al., 2009; Benner and Amon, 2015), the high percentage of *α*-gly, *β*-gly, glu-6 and di-P in the HMW portion would highlight their high reactivity and confirm those assumptions from the perspective of MW (Fig. 5). The results shown in this study therefore provide new

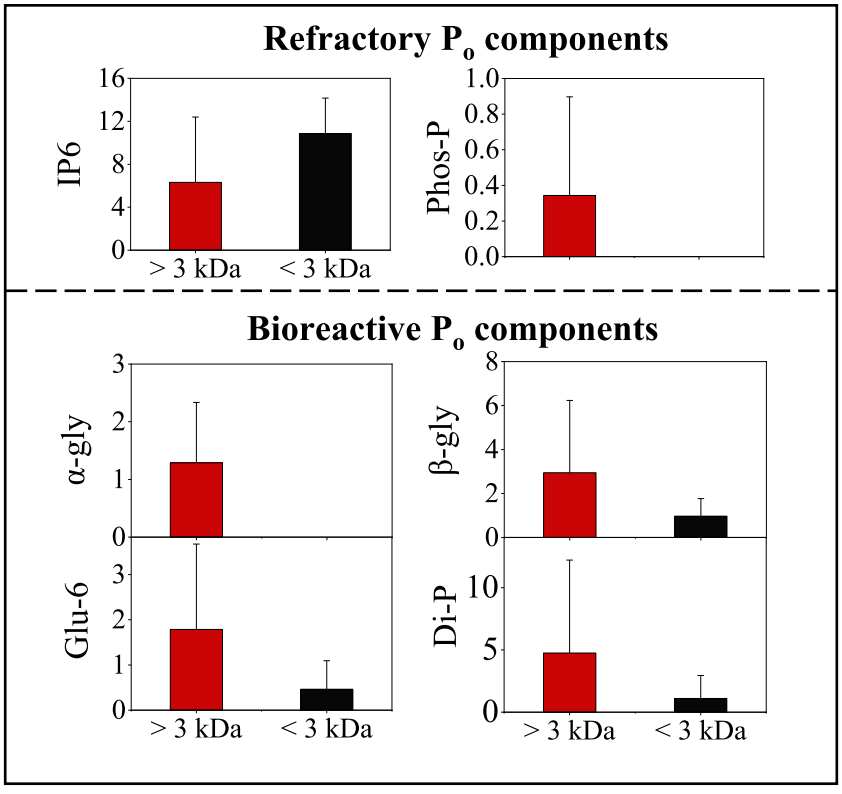

Fig. 5. Comparison of MW distribution of refractory and bioreactive P_o components.

evidence to explain the compositional heterogeneity and bioreactivity of sediment P_o from the perspective of MW.

Our findings highlight the strong heterogeneity in molecular size, chemical composition and bioreactivity of P_o in sediments. Previous studies mostly focused on the chemical transformations of P_o, while little attention was paid to the molecular size transformation of P_o from the perspective of MW. Future studies should focus on investigating molecular size and compositional transformation of P_o to better understand its bioreactivity, fate and environmental impact. For example, organic molecules can transform from the HMW fraction into the LMW one through disaggregation and biodegradation (Wang and Guo, 2001; Santschi et al., 2006), and then the LMW fraction is formed into HMW substances via colloidal pumping and self-assembly (Santschi, 2018; Xu and Guo, 2018). Studying the bioreactivity of P_o components in sediments with respect to different MWs is another urgent issue. To sum up, understanding the relationship between P_o components and their MW distribution might offer new or even breakthrough insights about the biogeochemical cycle of P. For this end, new methods are required to better characterize P_o molecular composition in sediments.

4. Conclusions

This study explored the compositional characteristics of P_o in sediments at molecular level by linking the MW distribution with different P_o components. Results showed that sediment P_o mainly consisted of mono-P (14±8.8% of NaOH-EDTA extractable total P on average), di-P (1.4±1.4%) and phos-P (0.1±0.1%), while the abundance of P_o was largely underestimated by using ^{31}P NMR method. Some species of mono-P were successfully identified, and the content of these species followed a decreasing order as: IHP6 > RNA-mnP > β-gly > Glu-6 > α-gly, which was largely dependent upon their bioreactivity. A significant relationship between MW distribution and P_o components was observed despite the great differences among sediment samples. For the refractory P_o components, IHP6 was mainly rich in MW < 3 kDa while phos-P was almost only detectable in the MW > 3 kDa, which might be due to the metal binding affinities. Due to microbial degradation and self-assembly, the abundance of bioreactive P_o species (α-gly, β-gly, Glu-6, di-P) in HMW (> 3 kDa) portions were all higher than that of LMW ones (< 3 kDa). If the HMW or colloidal ones were biologically and chemically more reactive than its LMW counterparts, the high percentage of α-gly, β-gly, glu-6 and di-P in the HMW portion would highlights their high reactivity from the perspective of MW. The insights derived from this study shed light on the further understanding of compositional characteristics of P_o in sediments.

Declaration of Competing Interest

The authors declared that they have no conflicts of interest to this work. We declare that we do not have any commercial or associative interest that represents a conflict of interest in connection with the work submitted in this article.

Acknowledgments

This research was jointly supported by National Natural Science Foundation of China (No. U1902207), Guangdong-Hong Kong Joint Laboratory for Water Security (2020B1212030005), Yunnan Key Laboratory of Pollution Process and Management of Plateau Lake-Watershed (2020-02-2-W2, 2020-124A-W2), National High-level Personnel of Special Support Program (People Plan, grant number 312232102).

Supplementary materials

Supplementary material associated with this article can be found, in the online version, at doi:10.1016/j.watres.2022.118197.

References

Ahlgren, J., Reitzel, K., Brabandere, H.D., Gogoll, A., Rydin, E., 2011. Release of organic P forms from lake sediments. Water Res. 45 (2), 565–572.
Ahlgren, J., Reitzel, K., Danielsson, R., Gogoll, A., Rydin, E., 2006a. Biogenic phosphorus in oligotrophic mountain lake sediments: Differences in composition measured with NMR spectroscopy. Water Res. 40 (20), 3705–3712.
Ahlgren, J., Reitzel, K., Tranvik, L., Gogoll, A., Rydin, E., 2006b. Degradation of organic phosphorus compounds in anoxic Baltic Sea sediments, a 31P nuclear magnetic resonance study. Limnol. Oceanogr. 51, 2341–2348.
Amon, R.M.W., Benner, R., 1994. Rapid cycling of high-molecular-weight dissolved organic matter in the ocean. Nature 369, 549–552.
Amon, R.M.W., Benner, R., 1996. Bacterial utilization of different size classes of dissolved organic matter. Limnol. Oceanogr. 41 (l), 41–51.
Arnosti, C., Repeta, D.J., Blough, N.V., 1994. Rapid bacterial degradation of polysaccharides in anoxic marine systems. Geochim. Cosmochim. Ac. 58, 2639–2652.
Barbara, J., Navaratnam, J.A., Walbridge, M.R., 2006. Characterizing dissolved and particulate phosphorus in water with ^{31}P nuclear magnetic resonance spectroscopy. Environ. Sci. Technol. 40 (24), 7874–7880.
Bedrock, et al., 1995. Effect of pH on precipitation of humic acid from peat and mineral soils on the distribution of phosphorus forms in humic and fulvic acid fractions. Commun. Soil. Sci. Plan. 26, 1411–1425.
Benner, R., Amon, R.M.W., 2015. The size-reactivity continuum of major bioelements in the ocean. Annu. Rev. Mar. Sci. 7, 185–205.
Björkman, K.M., Karl, D.M., 2003. Bioavailability of dissolved organic phosphorus in the euphotic zone at Station ALOHA, North Pacific Subtropical Gyre. Limnol. Oceanogr. 48 (3), 1049–1057.
Bowman, R.A., Cole, C.V., 1978. An exploratory method for fractionation of organic phosphorus from grassland soils. Soil Sci. 125 (2), 95–101.
Bünemann, E.K., Smernik, R.J., Doolette, A.L., Marschner, P., Stonor, R.N., Wakelin, S.A., McNeill, A.M., 2008. Forms of phosphorus in bacteria and fungi isolated from two Australian soils. Soil Biol. Biochem. 40 (7), 1908–1915.
Cade-Menun, B.J., 2005. Characterizing phosphorus in environmental and agricultural samples by 31P nuclear magnetic resonance spectroscopy. Talanta 66 (2), 359–371.
Cade-Menun, B.J., Preston, C.M., 1996. A comparison of soil extraction procedures for ^{31}P NMR spectroscopy. Soil Sci. 161 (11), 770–785.
Chen, W.B., Smith, D.S., Guéguen, C., 2013. Influence of water chemistry and dissolved organic matter (DOM) molecular size on copper and mercury binding determined by multiresponse fluorescence quenching. Chemosphere 92, 351–359.
Chinese Ecological Environment Bullet, 2018. www.mee.gov.cn/ywdt/tpxw/201905/t20190529_704841.shtml.
Christl, I., Kretzschmar, R., 2001. Relating ion binding by fulvic and humic acids to chemical composition and molecular size. 2. Metal binding. Environ. Sci. Technol. 35 (12), 2512–2517.
Ding, S.M., Bai, X.Z., Fan, C.X., Zhang, L., 2010. Caution needed in pretreatment of sediments for refining phosphorus-31 nuclear magnetic resonance analysis: results from a comprehensive assessment of pretreatment with ethylenediaminetetraacetic acid. J. Environ. Qual. 39 (1), 1668–1678.
Doolette, A., Smernik, R., Dougherty, W., 2009. Spiking improved solution phosphorus-31 nuclear magnetic resonance identification of soil phosphorus compounds. Soil. Sci. Soc. Am. J. 73 (3), 919–927.
Feng, W.Y., Wu, F.C., He, Z.Q., 2018. Simulated bioavailability of phosphorus from aquatic macrophytes and phytoplankton by aqueous suspension and incubation with alkaline phosphatase. Sci. Total. Environ 617, 1431–1439, 616.
Feng, W.Y., Zhu, Y.R., Wu, F.C., Meng, W., Giesy, J.P., He, Z.Q., Song, L.R., Fan, M.L., 2016. Characterization of phosphorus forms in lake macrophytes and algae by solution ^{31}P nuclear magnetic resonance spectroscopy. Environ. Sci. Pollut. Res. 23, 7288–7297.
Gao, S.X., Zhang, X., Fan, W.Y., Sheng, G.P., 2021. Molecular insight into the variation of dissolved organic phosphorus in a wastewater treatment plant. Water Res. 203, 117529.
Ged, E.C., Boyer, T.H., 2013. Molecular weight distribution of phosphorus fraction of aquatic dissolved organic matter. Chemosphere 91, 921–927.
Giles, C.D., Lee, L.G., Cade-Menun, B.J., Hill, J.E., Isles, P.D.F., Schroth, A.W., Druschel, G.K., 2015. Characterization of organic phosphorus form and bioavailability in lake sediments using ^{31}PNuclear Magnetic Resonance and enzymatic hydrolysis. J. Environ. Qual. 44 (3), 882–894.
Guo, L., White, D.M., Xu, C., Santschi, P.H., 2009. Chemical and isotopic composition of HMW-DOM from the Mississippi River plume. Mar. Chem. 114, 63–71.
He, Z.Q., Olk, D.C., Cade-Menun, B., 2011. Forms and lability of phosphorus in humic acid fractions of Hord silt loam Soil. Soil. Sci. Soc. Am. J. 75 (5), 1712–1722.
Horppila, J., 2019. Sediment nutrients, ecological status and restoration of lakes. Water Res. 160, 206–208.
Hupfer, M., Gächter, R., Rüegger, H., 1995. Polyphosphate in lake sediments: ^{31}P NMR spectroscopy as a tool for its identification. Limnol. Oceanogr. 40 (3), 610–617.
Hurtarte, L.C.C., Amorim, H.C.S., Kruse, J., Cezar, J.C., Klysubun, W., Prietzel, J., 2020. A novel approach for the quantification of different inorganic and organic phosphorus compounds in environmental samples by P $L_{2,3}$-edge x-ray absorption near-edge structure (XANES) spectroscopy. Environ. Sci. Technol. 54, 2812–2820.
Ivanoff, D.B., Reddy, K.R., Robinson, S., 1998. Chemical fractionation of organic phosphorus in selected histosols. Soil Sci. 163 (1), 36.
Jørgensen, C., Jensen, H.S., Andersen, F.Ø., Egemose, S., Reitzel, K., 2011. Occurrence of orthophosphate monoesters in lake sediments: Significance of myo-and scyllo-inositol hexakisphosphate. J. Environ. Monit. 13 (8), 2328–2334.

Kerner, M., Hohenberg, H., Ertl, S., Reckermann, M., Spitzy, A., 2003. Self-organization of dissolved organic matter to micelle-like microparticles in river water. Nature 422, 150–154.
Kurek, M.R., Harir, M., Shukle, J.T., Schroth, A.W., Schmitt-Kopplin, P., Druschel, G.K., 2020. Chemical fractionation of organic matter and organic phosphorus extractions from freshwater lake sediment. Anal. Chim. Acta. 1130, 29–38.
Lakshman, S., Mills, R., Patterson, H., Cronan, C., 1993. Apparent differences in binding site distributions and aluminum (III) complexation for three molecular weight fractions of a coniferous soil fulvic acid. Anal. Chim. Acta. 282 (1), 101–108.
Le, C., Zha, Y., Li, Y., Sun, D., Lu, H., Yin, B., 2010. Eutrophication of lake waters in China: cost, causes, and control. Environ. Manag. 45, 662–668.
Li, J.B., Xie, T., Zhu, H., Zhou, J., Li, C.N., Xiong, W.J., Xu, L., Wu, Y.H., He, Z.L., Li, X.Z., 2021. Alkaline phosphatase activity mediates soil organic phosphorus mineralization in a subalpine forest ecosystem. Geoderma 404, 115376.
Li, X.L., Guo, M.L., Duan, X.D., Zhao, J.W., Hua, Y.M., Zhou, Y.Y., Liu, G.L., Dionysiou, D. D., 2019. Distribution of organic phosphorus species in sediment profiles of shallow lakes and its effect on photo-release of phosphate during sediment resuspension. Environ. Int. 130, 104916.
Liu, J., Yang, J.J., Cade-Menun, B.J., Liang, X.Q., Hu, Y.F., Liu, C.W., Zhao, Y., Li, L., Shi, J.Y., 2013. Complementary phosphorus speciation in agricultural soils by sequential fractionation, solution ^{31}P nuclear magnetic resonance, and phosphorus k-edge x-ray absorption near-edge structure spectroscopy. J. Environ. Qual. 42, 1763–1770.
Makarov, M.I, Haumaier, L., Zech, W., 2002. Nature of soil organic phosphorus: An assessment of peak assignments in the diester region of ^{31}P NMR spectra. Soil Biol. Biochem. 34, 1467–1477.
McDowell, R.W., Cade–Menun, B., Stewart, I., 2007. Organic phosphorus speciation and pedogenesis: analysis by solution ^{31}P nuclear magnetic resonance spectroscopy. Eur. J. Soil Sci. 58 (6), 1348–1357.
McLaren, T.I., Simpson, R.J., McLaughlin, M.J., Smernik, R.J., McBeath, T.M., Guppy, C. N., Richardson, A.E., 2015a. An assessment of various measures of soil P and the net accumulation of P in fertilized soils under pasture. J. Plant. Nutr. Soil Sci. 178 (4), 543–554.
McLaren, T.I., Smernik, R.J., McLaughlin, M.J., McBeath, T.M., Kirby, J.K., Simpson, R. J., Guppy, C.N., Doolette, A.L., Richardson, A.E., 2015b. Complex forms of soil organic phosphorus−a major component of soil phosphorus. Environ. Sci. Technol. 49, 13238–13245.
Ni, Z.K., Wang, S.R., Wang, Y.M., 2016. Characteristics of bioavailable organic phosphorus in sediment and its contribution to lake eutrophication in China. Environ. Pollut. 219, 537–544.
Ni, Z.K., Xiao, M.Q., Luo, J., et al., 2021. Molecular insights into water-extractable organic phosphorus from lake sediment and its environmental implications. Chem. Eng. J. 416, 129004.
Orihel, D., Baulch, H., Casson, N.J., North, R.L., Parsons, C.T., Seckar, D.C.M., Venkiteswaran, J.J., 2017. Internal phosphorus loading in Canadian fresh waters: a critical review and data analysis. Can. J. Fish. Aquat. Sci. 74 (12), 2005–2029.
Paraskova, J.V., Rydin, E., Sjöber, P.J.R., 2013. Extraction and quantification of phosphorus derived from DNA and lipids in environmental samples. Talanta 115, 336–341.
Paytan, A., Cade-Menun, J.B., McLaughlin, K., Faul, K.L., 2003. Selective phosphorus regeneration of sinking marine particles: evidence from ^{31}P-NMR. Mar. Chem. 82, 55–70.
Read, E.K., Ivancic, M., Hanson, P., Cade-Menun, B.J., McMahon, K.D., 2014. Phosphorus speciation in a eutrophic lake by ^{31}P NMR spectroscopy. Water Res. 62, 229–240.
Reitzel, K., Ahlgren, J., DeBrabandere, H., Waldebäck, M., Gogoll, A., Tranvik, L., Rydin, E., 2007. Degradation rates of organic phosphorus in lake sediment. Biogeochemistry 82, 15–28.
Reitzel, K., Ahlgren, J., Gogoll, A., Rydin, E., 2006. Effects of aluminum treatment on phosphorus, carbon, and nitrogen distribution in lake sediment: a ^{31}P NMR study. Water Res. 40 (4), 647–654.
Rippey, B., Campbell, J., McElarney, Y., Thompson, J., Gallagher, M., 2021. Timescale of reduction of long-term phosphorus release from sediment in lakes. Water Res. 200, 117283.
Ruban, V., López-Sánchez, J.F., Pardo, P., Rauret, G., Muntau, H., Quevauviller, P., 1999. Selection and evaluation of sequential extraction procedures for the determination of phosphorus forms in lake sediment. J. Environ. Monit. 1 (1), 51–56.
Ruttenberg, K.C., Dyhrman, S.T., 2005. Temporal and spatial variability of dissolved organic and inorganic phosphorus, and metrics of phosphorus bioavailability in an upwelling-dominated coastal system. J. Geophys. Res. 110 (C10), 1–22.
Santschi, P.H., 2018. Marine colloids, agents of the self-cleansing capacity of aquatic systems: Historical perspective and new discoveries. Mar. Chem. 207, 124–135.
Santschi, P.H., Murray, J.W., Baskaran, M., Benitez-Nelson, C.R., Guo, L., Hung, C.C., Lamborg, C., Moran, S.B., Passow, U., Roy-Barman, M., 2006. Thorium speciation in seawater. Mar. Chem. 100, 250–268.
Shinohara, R., Imai, A., Kawasaki, N., Komatsu, K., Kohzu, A., Miura, S., Sano, T., Tomioka, N., 2012. Biogenic phosphorus compounds in sediment and suspended particles in a shallow eutrophic lake: a ^{31}P-nuclear magnetic resonance (^{31}P NMR) study. Environ. Sci. Technol. 46, 10572–10578.
Shinohara, R., Imai, A., Kohzu, A., Tomioka, N., Furusato, E., Satou, T., Sano, T., Komatsu, K., Miura, S., Shimotori, K., 2016. Dynamics of particulate phosphorus in a shallow eutrophic lake. Sci. Total. Environ. 563, 413–423, 564.
Silbernagel, R., Shehee, T.C., Martin, C.H., Hobbs, D.T., Clearfield, A., 2016. Zr/Sn(IV) phosphonates as radiolytically stable ion-exchange materials. Chem. Mater. 28, 2254–2259.
Søndergaard, M., Jensen, J.P., Jeppesen, E., 2003. Role of sediment and internal loading of phosphorus in shallow lakes. Hydrobiologia 506 (1–3), 135–145.
Suzumura, M., Ishikawa, K., Ogawa, H., 1998. Characterization of dissolved organic phosphorus in coastal seawater using ultrafiltration and phosphohydrolytic enzymes. Limnol. Oceanogr. 43, 1553–1564.
Tu, L., Gilli, A., Lotter, A., Vogel, H., Moyle, M., Boyle, J.F., Grosjean, M., 2021. The nexus among long-term changes in lake primary productivity, deep-water anoxia, and internal phosphorus loading, explored through analysis of a 15,000-year. Global Planet. Change 207, 103643.
Turner, B.L., Condron, L.M., Richardson, S.J., Peltzer, D.A., Allison, V.J., 2007. Soil organic phosphorus transformations during pedogenesis. Ecosystems 10 (7), 1166–1181.
Turner, B.L., Mahieu, N., Condron, L.M., 2003b. The phosphorus composition of temperate pasture soils determined by NaOHEDTA extraction and solution 31P NMR spectroscopy. Org. Geochem. 34, 1199–1210.
Turner, B.L., Mahieu, N., Condron, L.M., 2003a. Phosphorus-31 nuclear magnetic resonance spectral assignments of phosphorus compounds in NaOH-EDTA extracts. Soil Sci. Soc. Am. J. 67, 497–510.
Turner, B.L., McKelvie, I.D., Haygarth, P.M., 2002. Characterisation of water-extractable soil organic phosphorus by phosphatase hydrolysis. Soil. Biol. Biochem. 34 (1), 27–35.
Turner, B.L., Weckström, K., 2009. Phytate as a novel phosphorusspecific paleo-indicator in aquatic sediments. J. Paleolimnol. 42 (3), 391–400.
Venkatesan, A.K., Gan, W.H., Ashani, H., et al., 2018. Size exclusion chromatography with online ICP-MS enables molecular weight fractionation of dissolved phosphorus species in water samples. Water Res. 133, 264–271.
Wang, W.X., Guo, L., 2001. Production of colloidal organic carbon and trace metals by phytoplankton decomposition. Limnol. Oceanogr. 46 (2), 278–286.
Weng, G.G., Zheng, L.M., 2020. Chiral metal phosphonates: assembly, structures and functions. Sci. China Chem. 63, 619–636.
Worsfold, P.J., Monbet, P., Tappin, A.D., et al., 2008. Characterisation and quantification of organic phosphorus and organic nitrogen components in aquatic systems: a review. Anal. Chim. Acta. 624 (1), 37–58.
Wu, F.C., Xing, B.S., 2009. Natural organic matter and its significance in the environment. Beijing: Science Press (in Chinese).
Wu, Z.H., Wang, S.R., 2017. Release mechanism and kinetic exchange for phosphorus (P) in lake sediment characterized by diffusive gradients in thin films (DGT). J. Hazard. Mater. 331 (5), 36–44.
Xiong, L.P., Lv, K., Gu, M., Yang, C.T., Wu, F.C., Han, J., Hu, S., 2019. Efficient capture of actinides from strong acidic solution by hafnium phosphonate frameworks with excellent acid resistance and radiolytic stability. Chem. Eng. J. 355, 159–169.
Xu, H.C., Guo, L.D., 2018. Intriguing changes in molecular size and composition of dissolved organic matter induced by microbial degradation and self-assembly. Water Res. 135, 187–194.
Xu, H.C., Zou, L., Guan, D.X., Li, W.T., Jiang, H.L., 2019. Molecular weight-dependent spectral and metal binding properties of sediment dissolved organic matter from different origins. Sci. Total. Environ. 665, 828–835.
Yang, B., Lin, H., Bartlett, S.L., Houghton, E.M., Robertson, D.M., Guo, L.D., 2021. Partitioning and transformation of organic and inorganic phosphorus among dissolved, colloidal and particulate phases in a hypereutrophic freshwater estuary. Water Res. 196, 117025.
Zhang, L., Wang, S.R., Jiao, L.X., Ni, Z.K., Xi, H.Y., Liao, J.Y., Zhu, C.W., 2013. Characteristics of phosphorus species identified by ^{31}P NMR in different trophic lake sediments from the Eastern Plain. China. Ecol. Eng. 60, 336–343.
Zhang, L., Wang, S.R., Zhao, H.C., Li, Y.P., Huo, S.L., Qian, W.B., Yang, Y.L., Cheng, J., 2016. Using multiple combined analytical techniques to characterize water extractable organic nitrogen from Lake Erhai sediment. Sci. Total. Environ. 542, 344–353.
Zhang, W.Q., Shan, B.Q., Zhang, H., Tang, W.Z., 2014. Characterization and optimization of the NaOH-EDTA extracts for solution ^{31}P-NMR analysis of organic phosphorus in river sediments. Environ. Sci. 35 (1), 163–170 (in Chinese).
Zhang, W.Q., Zhu, X.L., Jin, X., et al., 2017. Evidence for organic phosphorus activation and transformation at the sediment–water interface during plant debris decomposition. Sci. Total. Environ. 583, 458–465.
Zhu, Y.R., Wu, F.C., He, J.Y., Guo, X.X., Qu, F.Z., Xie, J.P., Giesy, J.P., Liao, H.Q., Guo, F., 2013. Characterization of organic phosphorus in lake sediments by sequential fractionation and enzymatic hydrolysis. Environ. Sci. Technol. 47, 7679–7768.